JOURNAL OF MATERIALS SCIENCE 22 (1987) 2509–2514

Isothermal crystallization kinetics of $Ni_{60}Nb_{40-x}Cr_x$ glasses

D. AKHTAR, R. P. MATHUR
Defence Metallurgical Research Laboratory, Kanchanbagh, Hyderabad-500 258, India

Isothermal crystallization kinetics of $Ni_{60}Nb_{40-x}Cr_x$ (x = 0, 5, and 13 at%) glasses was investigated by differential scanning calorimetry. It was possible to separate out the kinetics of formation of various phases which are obtained on crystallization of these glasses. The results are compared with the earlier investigations [1] in which the data were obtained by constant heating rate experiments. The crystallization of M-phase, Ni_3Nb and $NbCr_2$ phases could be described by Johnson–Mehl–Avrami kinetics. The activation energies for the formation of these phases were found to decrease in the same order. A decreasing activation energy with increasing transformed fraction (time) was also observed. The results are interpreted in light of the values obtained for Avrami exponents.

1. Introduction

An understanding of the crystallization processes in metallic glasses is of prime technological importance since many physical and mechanical properties of these glasses are altered significantly on crystallization [2, 3]. Thermal analysis techniques such as differential scanning calorimetry (DSC) provide convenient methods for obtaining information on the transformation kinetics. The activation energy of crystallization has been frequently measured [1, 4–9] by the Kissinger method [10, 11] in which temperature shifts are monitored on heating the samples at selected rates in DSC. Literature [12, 13] on thermal analysis techniques, however, suggested that application of the Kissinger method to solid state reactions is improper. The recent work of Henderson [14] has provided a theoretical basis for the treatment of non-isothermal thermal analysis techniques and justifies use of the Kissinger method for many solid state transformations.

The activation energy, E, and Avrami exponent, n, have been evaluated in several cases [4, 15–22] using isothermal anneals in DSC. Unfortunately, in instances where crystallization involves more than one type of process, the isothermal exotherms associated with the individual processes invariably overlap [21], making difficult the task of estimation of the activation energies and Avrami exponents corresponding to the different processes. As a consequence, meaningful correlations between the kinetic data and the crystallization processes do not readily emerge in these cases. Although for certain metal–metalloid glasses, such correlations have been obtained, very few studies have been reported [17, 23] for metal–metal glasses.

Collins *et al.* [23] have evaluated the crystallization kinetics of $Ni_{60}Nb_{40}$ glass by the Kissinger method using DSC and through isothermal measurements of electrical resistivity. Akhtar and Chandrasekaran [24] have determined the glass formation range in the ternary $Ni_{60}Nb_{40-x}Cr_x$ alloys. Mathur and Akhtar [1] investigated the crystallization behaviour of $Ni_{60}Nb_{40-x}Cr_x$ glasses by X-ray diffraction and DSC measurements and estimated the activation energies of crystallization through the Kissinger method. In this paper, isothermal crystallization kinetics of these glasses are described. The Avrami exponents and activation energies have been evaluated by isothermal DSC experiments. It was possible to separate out the kinetics of formation of various crystalline phases which are obtained on crystallization of the $Ni_{60}Nb_{40-x}Cr_x$ glasses. The results are compared with the earlier investigations [1] to examine the data obtained by constant heating rate experiments.

2. Experimental procedure

Buttons of the $Ni_{60}Nb_{40-x}Cr_x$ (x = 0, 5, 10, and 13 at %) alloys were prepared by melting high-purity components in a non-consumable vacuum arc furnace under argon atmosphere. The buttons were repeatedly melted to ensure homogeneity. Amorphous ribbons were prepared by melt-spinning. Alloy buttons were cut into small pieces and remelted by induction heating in a quartz nozzle of $\sim$ 1 mm orifice diameter. The molten metal was ejected onto a rotating copper wheel ($\sim$ 200 mm diameter) using pure argon to provide the ejection pressure. The ribbons thus obtained were $\sim$ 20 to 25 μm thick and 2 to 3 mm wide.

DSC experiments were carried out in an advanced thermal analysis system, the computerized DuPont 1090. This instrument allows good control over the temperatures of isothermal scans. It heats up to the temperature set for isothermal scan at the maximum possible heating rate. Typically a temperature of 600° C could be arrived at in about 2 to 3 min time, starting from room temperature. The data could be stored, processed and compared, thus making it simple to produce comparative plots.

3. Results

3.1. Background

The crystallization behaviour of amorphous Ni_{60}-

0022–2461/87 $03.00 + .12

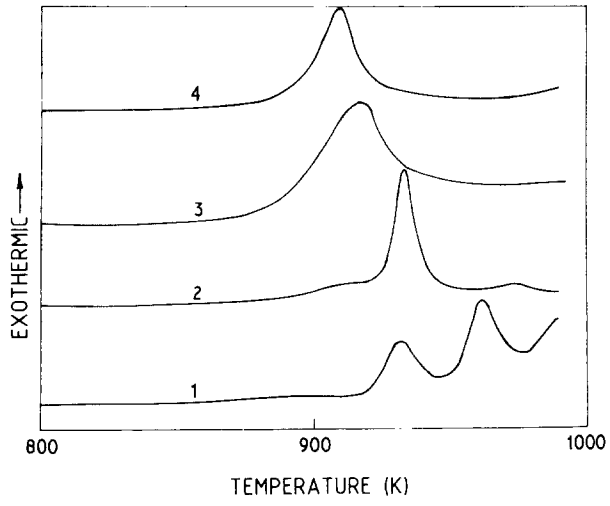

Figure 1 DSC thermograms obtained at a heating rate of 20 K min^{-1} for the amorphous $Ni_{60}Nb_{40-x}Cr_x$ alloys: (1) $x = 0$, (2) $x = 5$, (3) $x = 10$, and (4) $x = 13$.

$Nb_{40-x}Cr_x$ (x = 0, 5, 10 and 13 at %) alloys has recently been investigated by X-ray diffraction and continuous heating DSC experiments [1]. Typical DSC thermograms of the amorphous ribbons are reproduced in Fig. 1 at a heating rate of 20 K min^{-1}. The $Ni_{60}Nb_{40}$ glass was found to crystallize in three stages, Fig. 1 (curve 1); in the first stage the as-quenched glass partially crystallized into a metastable phase with structure similar to that of the M-phase in the ternary Ni–Nb–Al system. The second and third stages correspond to the formation of the equilibrium Ni_3Nb and NiNb phases, respectively. The first stage of crystallization of $Ni_{60}Nb_{40}$ glass was selected to investigate the isothermal kinetics of the formation of M-phase.

Since the exotherms of $Ni_{60}Nb_{40}$ glass are separated by a small temperature interval, separation of isothermal kinetics of the second and third stages of crystallization is rather complicated. Interestingly, on addition of 5 at % Cr, formation/stability of the M-phase is suppressed considerably and the $NbCr_2$ phase starts precipitating. Owing to the relatively small amounts of these two phases in $Ni_{60}Nb_{35}Cr_5$ alloy, the exotherms corresponding to the crystallization of these phases are weak, Fig. 1 (curve 2), and almost undetectable during isothermal annealing. The second stage corresponding to the formation of Ni_3Nb remains almost unaltered. The second stage of crystallization of $Ni_{60}Nb_{35}Cr_5$ glass was thus selected to study the kinetics of formation of Ni_3Nb phase.

As described earlier [1], the formation of M-phase is completely suppressed at 13 at % Cr and the third stage corresponding to the formation of NiNb phase also disappears completely at this composition. The single exotherm observed in the DSC thermogram of this alloy, Fig. 1 (curve 4), corresponds to the formation of both $NbCr_2$ and Ni_3Nb phases. It is shown later that separation of the kinetics of formation of $NbCr_2$ phase is possible at this composition. The broad exotherm observed for 10 at % Cr alloy, Fig. 1 (curve 3), corresponds to the formation of three phases – $NbCr_2$, Ni_3Nb and very little M-phase. This composition was therefore not investigated for isothermal kinetics. Further, kinetics of formation of NiNb phase (last stage of crystallization) could not be investigated due to limited operating temperature of the calorimeter.

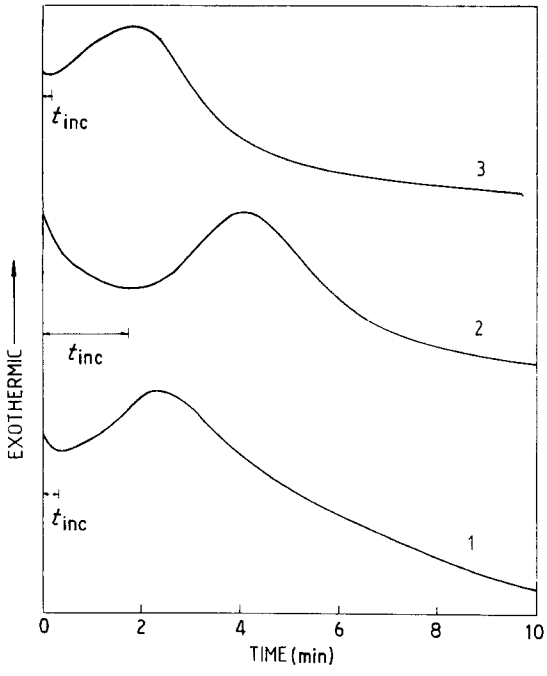

Figure 2 Typical exotherms obtained on isothermal annealing of amorphous (1) $Ni_{60}Nb_{40}$ at 907 K, (2) $Ni_{60}Nb_{35}Cr_5$ at 901 K, (3) $Ni_{60}Nb_{27}Cr_{13}$ at 880.5 K.

3.2. Results

Temperatures of isothermal anneals were selected after a few trial runs: (1) $Ni_{60}Nb_{40}$ glasses were annealed in the temperature range 896 to 907 K to determine the kinetics of formation of the M-phase, (2) $Ni_{60}Nb_{35}Cr_5$ glasses were annealed in the temperature range 901 to 911.5 K to determine the kinetics of formation of the Ni_3Nb phase and (3) $Ni_{60}Nb_{27}Cr_{13}$ glass ribbons were annealed in the temperature range 866.5 to 885 K to determine the kinetics of formation of both $NbCr_2$ and Ni_3Nb phases (which are separable subsequently). Anneals at higher temperatures could not be carried out because of the normally encountered difficulty of the incubation time falling short of the instrument transient time. At lower temperatures, because of slow transformation rates, the exotherms tended to flatten out. In the temperature ranges of investigations used, the base line became linear after the end of the instrument transient/completion of the previous crystallization stage and well defined isothermal exotherms could be obtained.

The incubation period was taken as the time interval between the specimen reaching the annealing temperature and the start of the transformation. The start of the transformation was taken as that instant at which the base line first deviated from linearity. Typical isothermal exotherms depicting the incubation period, t_{inc}, are shown in Fig. 2. Observation of a well defined incubation period for the second stage of $Ni_{60}Nb_{35}Cr_5$ glass, Fig. 2 (curve 2), was suggestive of the fact that the formation of $NbCr_2$/M-phase was completed before the annealing temperature was arrived at. The incubation times observed at some annealing

TABLE I Values of incubation times at some annealing temperatures

Composition	Temperature (K)	Incubation time (min)
$Ni_{60}Nb_{40}$	896	2.6
(M-phase)	901	1.3
	907	0.3
$Ni_{60}Nb_{35}Cr_5$	901	1.7
(Ni_3Nb phase)	905.5	1.0
	911.5	0.5
$Ni_{60}Nb_{27}Cr_{13}$	866.0	1.30
($NbCr_2$ + Ni_3Nb phases)	871.5	0.55
	873.0	0.45
	877.0	0.25
	880.5	0.20
	885.0	0

temperatures are listed in Table I for all the three compositions. A decrease in the incubation period with increasing annealing temperature is in keeping the fact that at temperatures below the nose of the time–temperature-transformation curve for crystalization, the nucleation rate increases with increasing temperature resulting in a decrease of incubation period [18].

Since the crystallization occurs by nucleation and growth, kinetics on isothermal annealing should be described by the Johnson–Mehl–Avrami equation [25]

$$x(t) = 1 - \exp(-bt^n) \quad (1)$$

where $x(t)$ is the fraction transformed at time t, b is a rate constant which depends on both the nucleation rate and the growth rate and n is the Avrami exponent that depends on the mechanism of crystallization. The fraction transformed, x at any time t, was determined as the ratio $A(t)/A(\text{tot})$ where $A(t)$ and $A(\text{tot})$ are the area under the isothermal exotherm up to time t and the total area of the exotherm, respectively. Plots of x against t at different temperatures yielded sigmoidal curves, shown in Figs 3, 4 and 5 for $Ni_{60}Nb_{40}$, $Ni_{60}Nb_{35}Cr_5$ and $Ni_{60}Nb_{27}Cr_{13}$ alloys, respectively.

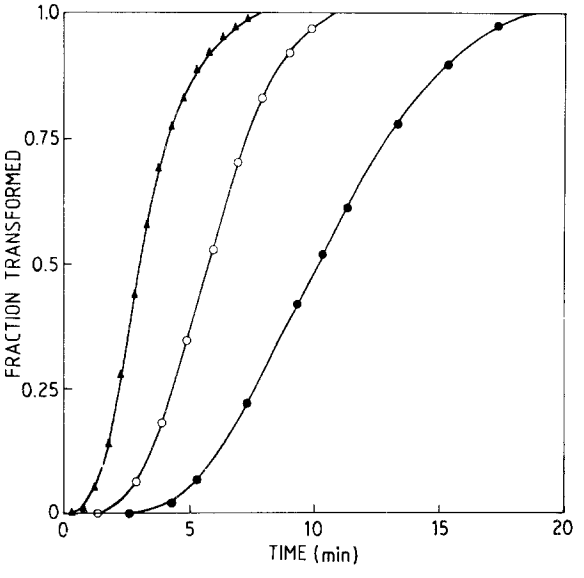

Figure 3 Sigmoidal curves depicting fraction transformed versus time elapsed at different temperatures for amorphous $Ni_{60}Nb_{40}$ alloy. (●) 896 K, (○) 901 K, (▲) 907 K.

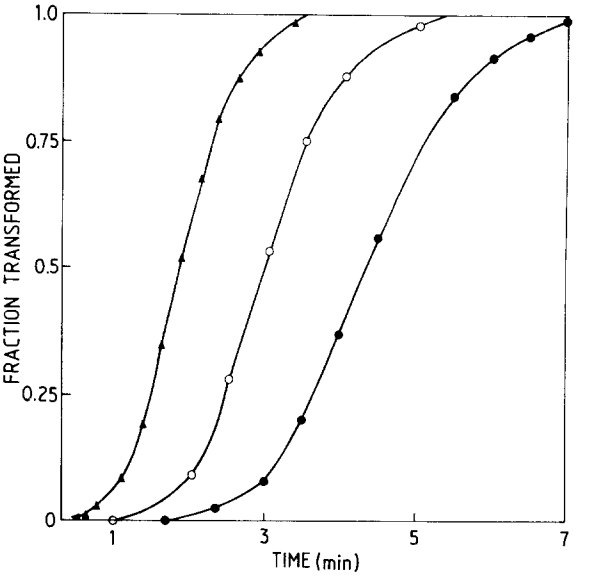

Figure 4 Sigmoidal curves depicting fraction transformed against time elapsed at different temperatures for amorphous $Ni_{60}Nb_{35}Cr_5$ alloy. (●) 901 K, (○) 905.5 K, (▲) 911.5 K.

The activation energy of the crystallization processes was evaluated from the isothermal exotherms, making use of the Arrhenius relation

$$t_x = t_0 \exp(E/RT) \quad (2)$$

where t_x is the time required for transformation of fraction x at temperature T and E is the activation energy. The plots of $\log t_x$ (x = 0.3, 0.5 and 0.8) against $1/T$ are shown in Figs 6, 7 and 8 for $Ni_{60}Nb_{40}$, $Ni_{60}Nb_{35}Cr_5$ and $Ni_{60}Nb_{27}Cr_{13}$ glasses, respectively. Calculated values of activation energy are also depicted in the figures.

Equation 1 can be rewritten as

$$\ln[-\ln(1 - x)] = \ln(b) + n \ln(t) \quad (3)$$

A plot of $\ln[-\ln(1 - x)]$ against $\ln(t)$ should yield a straight line with slope of n. Such plots are shown in Figs 9, 10 and 11 for $Ni_{60}Nb_{40}$, $Ni_{60}Nb_{35}Cr_5$ and

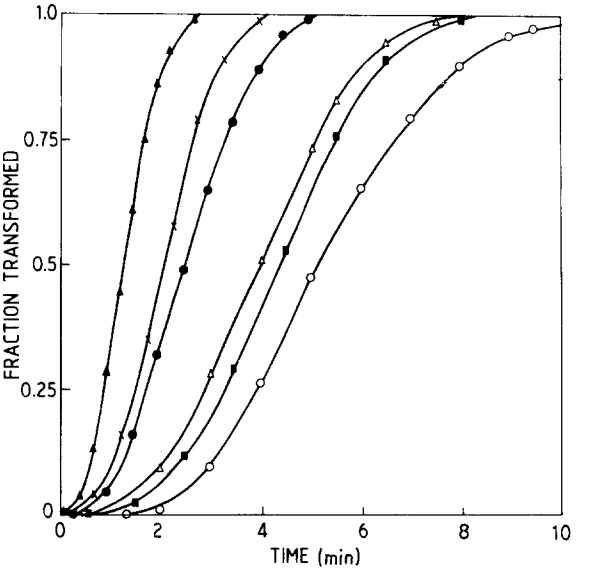

Figure 5 Sigmoidal curves depicting fraction transformed against time elapsed at different temperatures for amorphous $Ni_{60}Nb_{27}Cr_{13}$ alloy. (▲) 885 K, (×) 880.5 K, (●) 877 K, (△) 873 K, (■) 871.5 K, (○) 866.5 K.

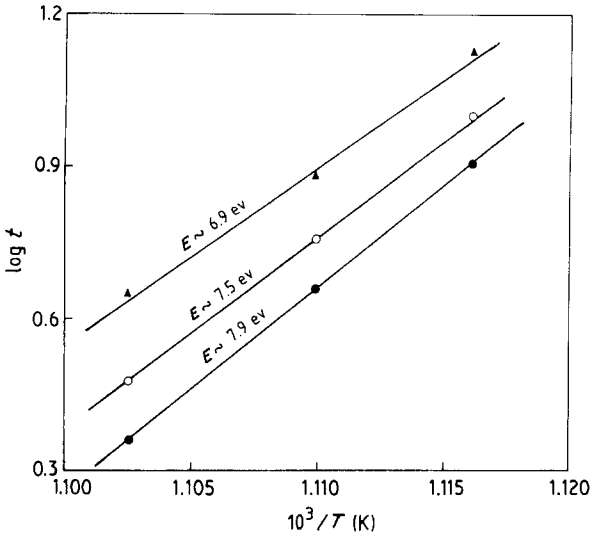

Figure 6 Plots of log t_x against $1/T$ for the estimation of activation energy for crystallization of M-phase in amorphous $Ni_{60}Nb_{40}$ alloy. (●) $t_{0.3}$, (○) $t_{0.5}$, (▲) $t_{0.8}$.

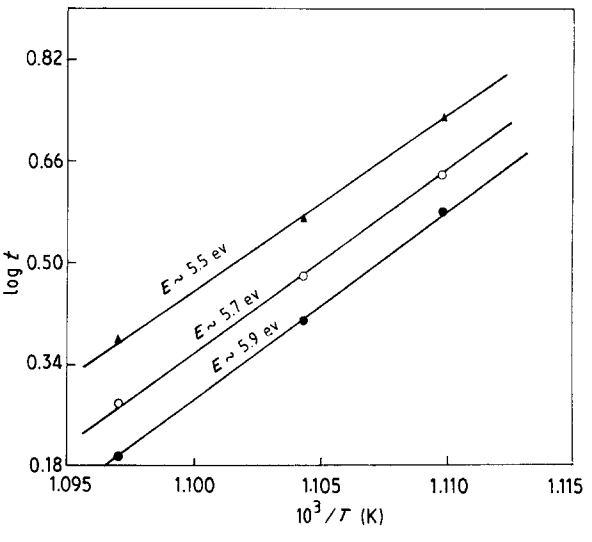

Figure 7 Plots of log t_x against $1/T$ for the estimation of activation energy for crystallization of Ni_3Nb phase in amorphous $Ni_{60}Nb_{35}Cr_5$ alloy. (●) $t_{0.3}$, (○) $t_{0.5}$, (▲) $t_{0.8}$.

$Ni_{60}Nb_{27}Cr_{13}$ glasses, respectively. Estimated values of the Avrami exponent, n are also depicted in these figures.

4. Discussion

The effective activation energy values estimated in the present investigations are compiled in Table II along with the values (appropriate for comparison) obtained by the authors by the Kissinger method [1]. Our activation energy value for the first stage crystallization of $Ni_{60}Nb_{40}$ determined through the Kissinger method, 5.8 eV, is somewhat lower than the value of 6.3 eV determined earlier [23, 26] by the same method. However, it is clear from Table II that the activation energies estimated through isothermal anneals are considerably larger than the values obtained by the Kissinger method. Greer [15] has determined the Curie temperature of nickel as a function of heating rate using DSC and observed that the apparent Curie temperature rises linearly with heating rate because of the increasing temperature lag of the sample. The lag was significant; ~6 to 8 K for the 80 K min^{-1} run. If no correction was made for the temperature lag, the experimental value of activation energy for crystallization of $Fe_{80}B_{20}$ glass was estimated to be 2.13 eV. On incorporation of correction for the temperature lag, the experimental value of activation energy was found to be 2.53 eV which was in agreement with the value of 2.49 eV derived from calculated transformation curves for various heating rates. Thus it was suggested that the activation energy values estimated through the Kissinger method are underestimated unless a correction for the temperature lag in DSC is incorporated. Since no such correction was applied in determining the activation energies in our earlier investigation, the reported [1] activation energies are underestimated; the cause of discrepancy in Table II thus becomes clear. Akhtar [4] has observed similar deviation in activation energies (estimated through isothermal and constant heating rate DSC experiments) for primary and polymorphic crystallization processes in the Metglas 2605 SC (Allied Corporation, USA). These observations support Greer's suggestion [15] that a correction for temperature lag in DSC should be incorporated in calculations of activation energy by the Kissinger method.

The plots of log t against $1/t$ in Figs 6 and 7 fit to single straight lines whereas the data in Fig. 8 do not. Separation of the data in Fig. 8 into two Arrhenius lines is somewhat questionable. However, it should be noted that the high-temperature region in Fig. 8 yields an activation energy of 5.6 eV which is very close to the values of 5.5 to 5.7 eV estimated for crystallization of Ni_3Nb phase from Fig. 7. Further, it has already been demonstrated [1] that the $NbCr_2$ phase crystallizes at a lower temperature than the Ni_3Nb phase; the temperature interval is perhaps too small to be separated in a continuous heating DSC run. Thus an average activation energy of 3.5 eV is obtained through the Kissinger peak shift method. On isothermal annealing in the temperature range 866.5 to 885 K, the isotherms at lower temperatures (866.5 to 873 K) appear to represent the crystallization behaviour of $NbCr_2$ phase with an Arrhenius slope yielding an

TABLE II Values of activation energies (in eV) estimated by the Kissinger method [1] and by isothermal anneals (present work)

Composition	Phase crystallizing	Kissinger method (peak position)	Isothermal anneals		
			$x = 0.3$	$x = 0.5$	$x = 0.8$
$Ni_{60}Nb_{40}$	M-phase	5.8	7.9	7.5	6.9
$Ni_{60}Nb_{35}Cr_5$	Ni_3Nb	4.0	5.9	5.7	5.5
$Ni_{60}Nb_{27}Cr_{13}$	Ni_3Nb	3.5	5.6	5.6	5.6
	$NbCr_2$		2.8	2.8	2.8

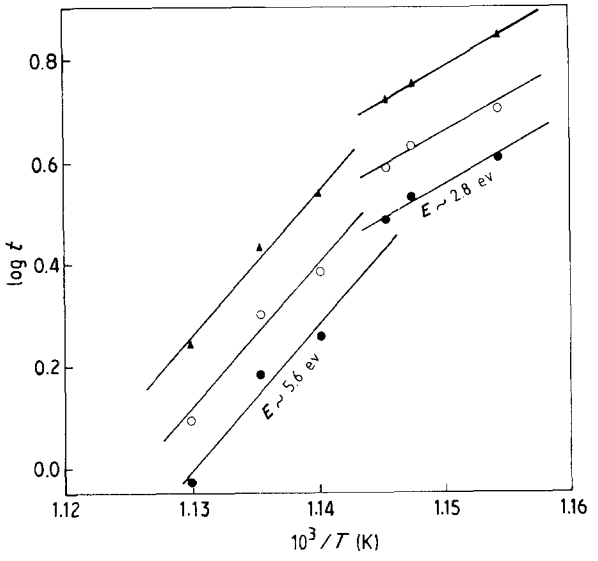

Figure 8 Plots of log t_x against $1/T$ for the estimation of activation energy for crystallization of Ni_3Nb and $NbCr_2$ phases in amorphous $Ni_{60}Nb_{27}Cr_{13}$ alloy. (●) $t_{0.3}$, (○) $t_{0.5}$, (▲) $t_{0.8}$.

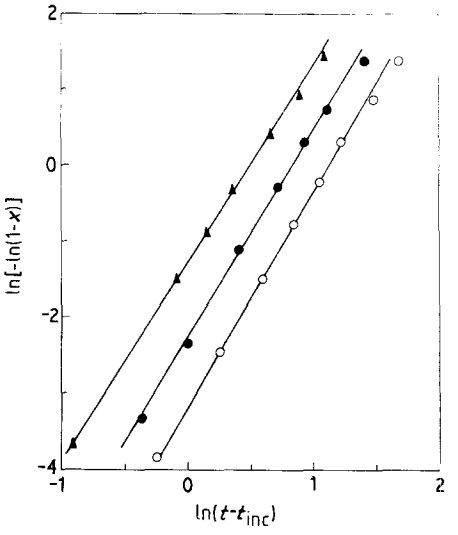

Figure 10 Plots of ln [− ln (1 − x)] against ln (t − t_{inc}) at different temperatures for evaluation of the Avrami exponent for crystallization of Ni_3Nb phase in amorphous $Ni_{60}Nb_{35}Cr_5$ alloy. (▲) 911.5 K, n = 2.7, (●) 905.5 K, n = 2.8, (○) 901 K, n = 2.9.

activation energy of 2.8 eV (Fig. 8). The isotherms at high temperatures (877 to 885 K) reveal a different Arrhenius slope yielding activation energy of 5.6 eV corresponding to the crystallization of Ni_3Nb phase. Thus the separation of Fig. 8 into two Arrhenius regions is considered reasonable.

The value of Avrami exponent n = 2.3 for the crystallization of M-phase is considerably higher than the average n value of 1.3 reported by Collins *et al.* [23]. However, our n value is similar to the n values observed during crystallization of many other metallic glasses [4, 15, 17, 22]. It may be noted that considerably erroneous values of n are obtained as a result of small errors in the analysis [18]. Collins *et al.* [23] have employed resistance measurement techniques to determine transformation rates by assuming that the fraction transformed was directly proportional to the change in resistance. Such an assumption is doubtful since in instances where small crystallites grow and still remain embedded in the amorphous matrix, change in resistance may not represent the transformation process entirely. It appears that the n values obtained by Collins *et al.* [23] are rather underestimated, the random spread in the n values for different temperatures obtained by the authors is perhaps a consequence of an error in the analysis. Indeed, very large deviations have been observed [15] in the n values estimated by various investigators for crystallization of $Fe_{80}B_{20}$ glass by the resistance measurement technique.

An unambiguous interpretation of the value of n can be obtained only by parallel microstructural investigations and independent measurements of the nucleation and growth rates. Unfortunately, thin foils for TEM examination could not be prepared with sufficiently uniform thickness to allow determination of the nucleation and growth rates. Let us consider the

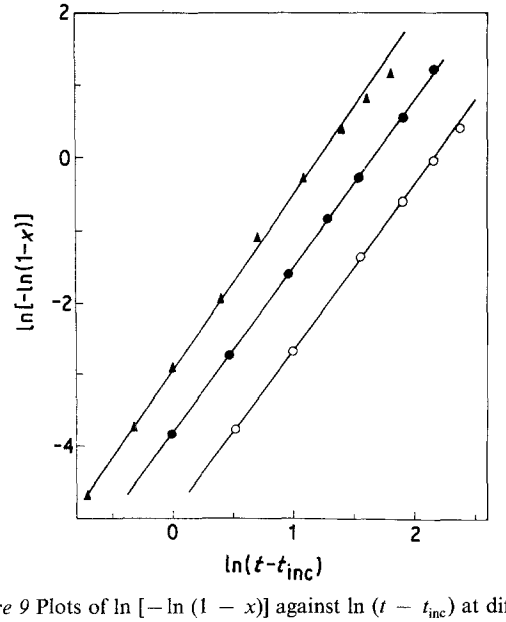

Figure 9 Plots of ln [− ln (1 − x)] against ln (t − t_{inc}) at different temperatures for evaluation of the Avrami exponent for crystallization of M-phase in amorphous $Ni_{60}Nb_{40}$ alloy. (▲) 907 K, n = 2.4, (●) 901 K, n = 2.3, (○) 896 K, n = 2.3

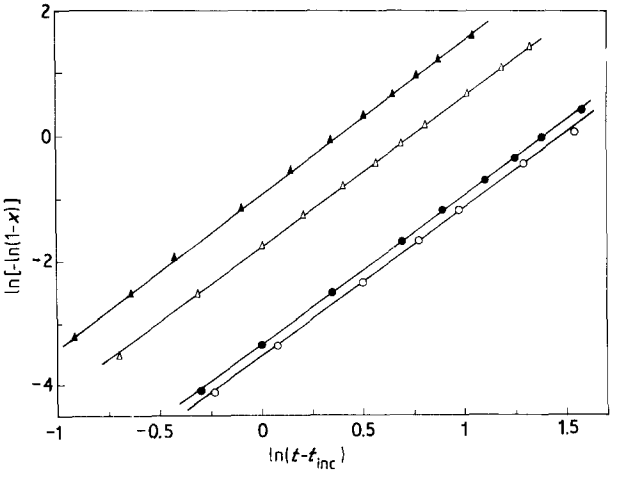

Figure 11 Plots of ln [− ln (1 − x)] against ln (t − t_{inc}) at different temperatures for evaluation of the Avrami exponent for crystallization of Ni_3Nb and $NbCr_2$ phases in amorphous $Ni_{60}Nb_{27}Cr_{13}$ alloy. (▲) 885 K, n = 2.5, (△) 880.5 K, n = 2.4 (●) 873 K, n = 2.4 (○) 866.5 K, n = 2.4.

expression for n [27]

$$n = a + pd \quad (4)$$

where $p = 1$ for linear growth, $p = 1/2$ for parabolic growth; $d = 1, 2$ or 3 for one, two or three dimensional growth; $a = 0$ for no nucleation (i.e. zero nucleation rate), $a = 1$ for constant nucleation rate, $0 < a < 1$ for a decreasing nucleation rate and $a > 1$ for an increasing nucleation rate. Our average n value of 2.3 for the crystallization of M-phase is thus indicative of a process involving nucleation at a decreasing rate with time and a parabolic growth. The average n value of 2.8 for crystallization of Ni_3Nb phase in $Ni_{60}Nb_{35}Cr_5$ glass would imply a nucleation rate which increases with time and parabolic growth. However, Greer [15] has suggested that the experimentally evaluated Avrami exponent falls short of the actual value because of certain instrumental and theoretical factors (Greer obtained a value of 2.8 for the Avrami exponent using isothermal DSC while the expected value was 3).

It should be noted in Table II that the value of activation energy E, decreases with increase in the fraction transformed, x. Ranganathan and von Heimendahl [28] have proposed a relationship

$$E = [n_n E_n + n_g E_g]/n \quad (5)$$

where subscripts n and g correspond to nucleation and growth, respectively. The activation energies for nucleation, E_n have been found [2] to be considerably higher than the activation energies for growth, E_g in the same glass. The decrease of activation energy of the total process, E, with transformed fraction (or time) thus implies that nucleation rate is decreasing with time. Our n value of 2.3 for crystallization of M-phase which indicates a decreasing nucleation rate and parabolic growth thus appears reasonable. On the other hand the n value of 2.8 for crystallization of Ni_3Nb phase in $Ni_{60}Nb_{35}Cr_5$ glass, which would imply an increasing nucleation rate with time becomes uncertain. If the observations of Greer [15] are considered in this case, the Avrami exponent will be modified to a value of 3 (or a value between 3 and 4), indicating a zero nucleation rate (or a nucleation rate decreasing with time) and a linear growth process. The first possibility is likely in $Ni_{60}Nb_{27}Cr_{13}$ glass considering the fact that the activation energy for crystallization of Ni_3Nb phase remains constant with increasing transformed fraction, x in this alloy whereas the second possibility holds for $Ni_{60}Nb_{35}Cr_5$ glass in which the activation energy decreases with increasing x. The n values estimated for crystallization processes in the $Ni_{60}Nb_{27}Cr_{13}$ alloy should, however, be interpreted with caution since the possibility of an error in estimation of these values can not be ruled out, as pointed out earlier.

5. Conclusions

It has been demonstrated that the activation energies obtained by isothermal DSC experiments are higher than those obtained by the Kissinger method. The observation is attributed to an underestimation of activation energies by the Kissinger method without incorporation of a correction for temperature lag in the DSC. It was possible to separate out isothermal kinetics of the formation of distinct crystalline phases which are obtained on crystallization of $Ni_{60}Nb_{40-x}Cr_x$ glasses. The activation energies for the formation of M-phase, Ni_3Nb and $NbCr_2$ phases decrease in the same order, reflecting ease of formation of $NbCr_2$ phase as compared to the M-phase when chromium is added to $Ni_{60}Nb_{40}$ alloy. The estimated Avrami exponents imply a decreasing (with time) nucleation rate and parabolic growth for the crystallization of M-phase. A zero (or decreasing with time) nucleation rate and linear growth process are indicated by the observed Avrami exponents for the formation of Ni_3Nb phase.

Acknowledgements

It is a pleasure to thank Professor P. Rama Rao for encouragement and permission to publish this work.

References

1. R. P. MATHUR and D. AKHTAR, *J. Mater. Sci.* **22** (1987) 683.
2. F. E. LUBORSKY (ed) "Amorphous Metallic Alloys" (Butterworths Monographs in Materials, 1983).
3. T. R. ANANTHARAMAN (ed) "Metallic Glasses, Production, Properties and Applications" (Trans. Tech. Publications, Switzerland, 1984).
4. D. AKHTAR, *Scripta Metall.* **20** (1986) 983.
5. D. AKHTAR, R. D. K. MISRA and S. B. BHADURI, *Acta Metall.* **34** (1986) 1307.
6. H. O. K. KIRCHNER, *Mater. Sci. Eng.* **23** (1976) 95.
7. F. E. LUBORSKY and H. H. LIEBERMANN, *Appl. Phys. Lett.* **33** (1978) 233.
8. J. C. SWARTZ, R. KOSSOWSKY, J. J. HAUGH and R. F. KRAUSE, *J. Appl. Phys.* **52** (1981) 3324.
9. K. H. J. BUSCHOW, *J. Appl. Phys.* **52** (1981) 3319.
10. H. E. KISSINGER, *J. Res. Nat. Bur. Std.* **57** (1957) 217.
11. *Idem, Anal. Chem.* **29** (1957) 1702.
12. R. C. MACKENZIE (ed) "Differential Thermal Analysis", Vol. 2 (Academic Press, New York, 1972).
13. W. W. WENDLANT, "Thermal Methods of Analysis", 2nd Edn. (Wiley, New York, 1974).
14. D. W. HENDERSON, *J. Non-Cryst. Solids* **30** (1979) 301.
15. A. L. GREER, *Acta Metall.* **30** (1982) 171.
16. L. V. MEISEL and P. J. COTE, *Acta Metall.* **31** (1983) 1053.
17. G. K. DEY and S. BANERJEE, *Mater. Sci. Eng.* **76** (1985) 127.
18. M. G. SCOTT and P. RAMACHANDRARAO, *ibid.* **29** (1977) 137.
19. E. COLEMAN, *ibid.* **23** (1976) 161.
20. M. G. SCOTT, *J. Mater. Sci.* **13** (1978) 291.
21. C. P. CHOU and D. TURNBULL, *J. Non-Cryst. Solids* **17** (1975) 169.
22. E. G. BABURAJ, G. K. DEY, M. J. PATNI and R. KRISHNAN, *Scripta Metall.* **19** (1985) 305.
23. L. E. COLLINS, N. J. GRANT and J. B. VANDER SANDE, *J. Mater. Sci.* **18** (1983) 804.
24. D. AKHTAR and V. CHANDRASEKARAN, *J. Mater. Sci. Lett.* **4** (1985) 1465.
25. J. BURKE, "Kinetics of Phase Transformation in Metals", (Pergamon Press, New York, 1965).
26. N. A. PRATTEN and M. G. SCOTT, *Scripta Metall.* **12** (1978) 137.
27. J. W. CHRISTIAN, "The Theory of Transformations in Metals and Alloys", 2nd Edn. (Pergamon Press, Oxford, 1975).
28. S. RANGANATHAN and M. VON HEIMENDAHL, *J. Mater. Sci.* **16** (1981) 2401.

Received 18 August
and accepted 15 December 1986